Analysis of Digital Filtering Design Based on Surface EMG Signals

2023 IEEE 3rd International Conference on Electronic Communications, Internet of Things and Big Data (ICEIB) | 979-8-3503-3386-2/23/$31.00 ©2023 IEEE | DOI: 10.1109/ICEIB57887.2023.10170168

Zeyu Xiao
School of Opto-Electronic and Communications Engineering, Xiamen University of Technology
Xiamen, China

Hanxin Shen*
School of Opto-Electronic and Communications Engineering, Xiamen University of Technology
Xiamen, China
hxshen@xmut.edu.cn

Hao Zhu
School of Opto-Electronic and Communications Engineering, Xiamen University of Technology
Xiamen, China

Jiaxiang Ye
School of Opto-Electronic and Communications Engineering, Xiamen University of Technology
Xiamen, China

Siyu Deng
School of Opto-Electronic and Communications Engineering, Xiamen University of Technology
Xiamen, China

Han Xiao
School of Opto-Electronic and Communications Engineering, Xiamen University of Technology
Xiamen, China

***Abstract*—The Butterworth IIR digital filter is designed to replace the high-cost analog filter to obtain a desirable surface EMG signal by addressing both the noise of the original surface EMG signal (SEMG) in the industrial frequency interference and baseline drift. The digital filtering design includes a 50 Hz I.F. trap and high-and low-pass digital filters. Experimental results show that the filtering process achieves -60 dB trap attenuation at 50 Hz and effectively filters out both high-and low-frequency signals, which supports the subsequent miniaturization of EMG bio-devices.**

Keywords—surface EMG signal, signal acquisition, IIR digital filtering, fast Fourier transform

I. Introduction

The surface EMG signal is a collection of potential changes obtained on the skin surface during muscle contraction, which represents the neuromuscular activity. Surface EMG signal detection is a noninvasive detection method, which has important significance in clinical diagnosis, rehabilitation medicine, and intelligent prosthesis control [1]. SEMG signals are usually weak with a voltage range generally between -5 and +5 mv [2], and its main energy part is concentrated within the frequency band of 20 to 500 Hz. Most signals are concentrated between 50 and 150 Hz. In addition, SEMG signals are easily interfered with by other signals, which affects the data fidelity of EMG signals and makes the information blurred. Therefore, in order to filter out various noises and obtain the required information, the acquired EMG signals need to be digitally filtered or analog filtered.

The designed filters are tested through numerical simulations and quantitative analysis using root mean square error (RMSE) to compare with the existing filters. The experimental results show that the performance of digital filters is superior to analog filters [3]. In addition, tests using recorded Biopac system signals showed RMSEs of 0.05665 and 0.05224 for the analog and digital filters, respectively [4]. Since the accuracy of analog filters is affected by the choice of passive component values, tolerances, manufacturing defects, and performance degradation [5], digital filters are superior to analog filters.

Most of the surface EMG acquisition devices produced contain separated components such as capacitors, inductors, and resistors to construct analog filter circuits [6]. This approach not only increases the circuit complexity but also leads to an oversized and unportable device. Due to the above problems, there is a wide range of applications to replace the original analog filters with digital filters to remove industrial frequency interference and baseline drift.

II. Design of Digital Filters

A. Principle of Operation

The digital filter calculates the signal according to the program for filtering. According to programs for the storage of digital filters, various filtering functions can be implemented. For digital filters, adding functions means adding programs without adding components without being affected by component errors, and processing the signal without increasing the size of the chip. The use of digital filtering methods solves the problems of analog filters limited by components [7]. A digital filter is an algorithm or device consisting of a digital multiplier, an adder, and a delay unit. The function of a digital filter is to perform arithmetic processing on the digital code of the input discrete signal to change the spectrum of the signal.

In this study, the acquired EMG signals are filtered by IIR high-pass and low-pass digital filters and IIR digital traps. IIR filters, i.e. infinite impulse response filters, have a unit impulse response of infinite length with a system transfer function.

$$\mathrm{H(z)}=\frac{\sum_{i=0}^{M} b_i z^{-i}}{1-\sum_{l=1}^{N} a_l z^{-l}}=\frac{Y(z)}{X(z)} \tag{1}$$

Its corresponding system differential equation is given by

$$y(n)=\sum_{i=0}^{M} x(n-i)b(i)+\sum_{l=1}^{N} y(n-l)a(l) \tag{2}$$

where *x(n)* is the system input and *y(n)* is the system output.

B. Design of Digital Filters

Infinite impulse response filters (IIR) have high filtering efficiency and require significantly lower filter orders than FIR filters for the same amplitude-frequency response conditions. Also, the design of IIR filters takes advantage of the results of analog filter design. IIR filters can obtain better filter amplitude-frequency characteristics with fewer

hardware resources. A significant feature of IIR filters is that they do not have strict linear phase characteristics and have significant performance advantages when strict linear phase characteristics are not required [8]. The conditions that need to be satisfied for a digital filter that theoretically satisfies engineering applications are obtained by design comparison with the FilterDesign tool in Matlab as shown in Table I.

TABLE I. DIGITAL FILTER DESIGN SPECIFICATIONS

Sampling rate	*Trap frequency*	*Frequency range after filtering*	*Spectral resolution*
10k	50Hz	20Hz~500Hz	0.33Hz

The higher the order of the same filter, the better the filtering effect. However, the higher the order, the higher the cost, and the larger the signal group delay. If the FIR filter is designed, the order is tens of hundreds of times higher than that of the IIR filter although it has a linear phase, and the computational requirements are high [9]. IIR filter not only achieves good attenuation in the passband and stopband but also obtains accurate edge frequencies in the passband and stopband, and the computational requirements are small, which largely reduces the hardware cost requirements. The IIR Butterworth filter requires only 14 steps to achieve a maximum attenuation of -100 dB at 50Hz, so the IIR Butterworth filter is designed for simulation.

The Butterworth filter is characterized by a relatively smooth frequency response curve in the passband [10]. The simulated low-pass Butterworth function is used as the system function of the filter, and its magnitude squared function is expressed as

$$|H_a(j\Omega)|^2 = \frac{1}{1+\varepsilon^2(\frac{j\Omega}{j\Omega_c})^{2N}} \tag{3}$$

where N is a positive integer indicating the order of the filter and Ω_c is the passband cutoff frequency 3 dB bandwidth (when ε = 1). Compared to other analog filters, the Butterworth filter has the flattest amplitude characteristics in the passband, i.e., the first 2N-1 order derivatives of the amplitude squared function of the Nth order low-pass filter at equal to 0. The attenuation in the stopband decreases monotonically with increasing frequency. The characteristics of the filter are completely determined by the order. As the order increases, the passband is flatter and closer to the ideal low-pass filter characteristics.

Usually, in the design of analog low-pass filters, technical specifications have bandpass cutoff frequency, the maximum attenuation in the passband Ap (dB), the cutoff frequency of the stopband, and the minimum attenuation in the stopband As (dB). The minimum order of the filter can be directly calculated by the following equation.

$$N \geq \frac{\lg(\lambda/\varepsilon)}{\lg(\Omega_s/\Omega_c)} \tag{4}$$

where

$$\varepsilon = \sqrt{(10^{0.1A_p}-1)} \tag{5}$$

$$\lambda = \sqrt{10^{0.1A_s}-1} \tag{6}$$

After obtaining the order of the Butterworth filter, the poles of the system function can be found according to the following equation.

$$s_{pk} = -\sin(\frac{2k-1}{2N}\pi) + j\cos(\frac{2k-1}{2N}\pi) \tag{7}$$

The frequency characteristics of the Butterworth filter vary monotonically with frequency in both the passband and the interior of the blocking band. The indicator at the edge of the passband satisfies the design requirement in the interior of the passband, thus resulting in a relatively high order of the filter. If the index accuracy is uniformly distributed throughout the passband or in the resistive band or both the passband and resistive band, the filter meets the design requirements, and the order is relatively low. This requires the approximation function to have equal ripple characteristics. Chebyshev I filter in the passband amplitude characteristics is equal ripple, but in the stopband, it is monotonic. Chebyshev type II has the opposite performance, monotonic in the passband and equal ripple in the stopband.

C. 50Hz Industrial Frequency Trap Design

The 50 Hz trap filter is equivalent to a 49 Hz low-pass filter and a 51 Hz high-pass filter. Hd(ejw) is an ideal low-pass filter with unit gain and linear phase in the band-pass and zero-response frequency bands. It is expressed in the form of (8).

$$H_d(e^{jw}) = \begin{cases} 1*e^{-j\alpha\omega}, & |\omega| \leq |\omega_c| \\ 0, & \omega_c \leq |\omega| \leq \pi \end{cases} \tag{8}$$

Figure 1 is an amplitude-frequency response plot describing the response of the system to input signals of different frequencies with frequency as the x-axis and amplitude response as the y-axis. The plot is used to represent the gain and attenuation characteristics of the system. It shows that the designed trap has -60 dB attenuation at 50 Hz, which meets the design needs. The standard EMG biofeedback instrument uses a 50Hz trap and a common mode rejection ratio of -50dB is sufficient, while the national industry standard is -26dB. Figure 2 illustrates the phase frequency response plot for describing the phase response of the system to input signals of different frequencies. In this case, the y-axis represents the phase response, which reflects the delay characteristics of the system. The filter is nonlinear but the overall trend of the time domain waveform before and after filtering remains the same.

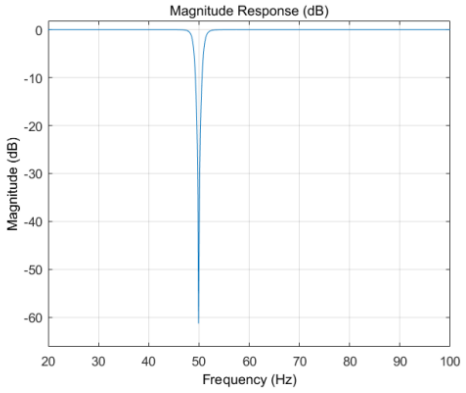

Fig. 1. Amplitude frequency response graph.

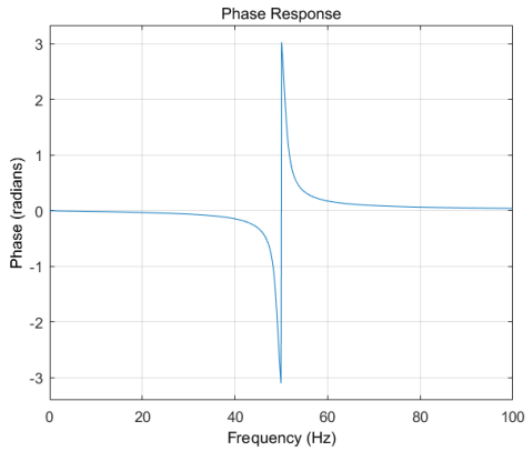

Fig. 2. Phase frequency response diagram.

III. Design of Surface EMG Collector Based on Digital Filtering Technology

A. Acquisition and Analysis System Design

The overall design flowchart of the surface EMG acquisition system is shown in Fig.. 3. The system converts the mains power (220V) to DC +9V supply through the power adapter. To ensure the normal operation of the STM32F4 chip, LM1117-3.3 output +3.3V is selected as the working power supply for the STM32 chip. MAX660 output -5V voltage and LM2576-5 output +5V voltage are used as the power supply for each chip in the EMG acquisition module. As the surface EMG signal is weak, the amplitude of EMG can reach 1−3 mV for healthy people, and the amplitude is generally less than 0.35 mV for people with residual limbs. Thus, the system adopts AD8220 differential amplifier chip to improve the input impedance and reduce the common mode interference, and the amplification is 200 times. After the operational amplifier amplification, the small EMG signal needs to be isolated from the post-stage circuit through the isolation device, and the HCNR201 optical coupling is used for the analog signal isolation transmission design.

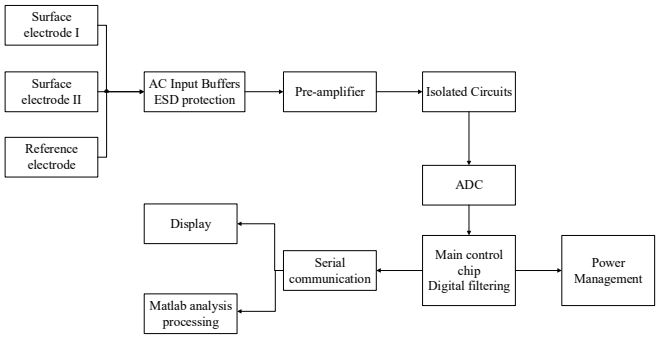

Fig. 3. Acquisition system design flow chart.

Since this experiment requires a high sampling rate and accurate sampling data storage, ordinary microcontrollers are no longer able to meet the demand. Therefore, the STM32F4 high-performance microcontroller is selected as the hardware chip for sampling in this system. ARM's Cortex-M4 processor strengthens the computing capability based on M3 with new floating point, DSP, and parallel computing. It has easy-to-use control and signal processing functions, low power consumption, and low cost, which is suitable for the experimental needs of this design.

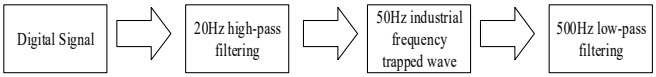

Fig. 4. Digital filtering flow chart of surface EMG signal.

The digital surface EMG signal processing flow chart is shown in Fig. 4. EMG acquisition devices [10] are analog filtered by hardware circuitry. First, the surface EMG signal is acquired by electrode sensors and subsequently amplified by a pre-amplification circuit. Then, it goes through high-pass filtering, low-pass filtering, secondary amplification, and then through IFE trapping, and finally the output waveform. The hardware digital filtering technique designed in this study is to convert the analog signal into a digital signal by AD conversion. The FFT spectrum analysis is performed to find the noise frequency point, then the MCU with the DSP function is used to perform digital high-pass filtering, trapping, and low-pass filtering and transmit the data through the serial port for the analysis and verification of the results of surface EMG signal on MATLAB.

B. Validation

Firstly, the electrode sheet acquires the forearm surface EMG signal, and then AD converts the digital signal to obtain a series of digital signals. Then, the coefficients of the designed IIR filter are exported through MATLAB's filterDesigner toolbox, and then the filter program is written in the keil5 platform. The DSP library is used to call the packaged arm_biquad_cascade_function. df1_f32 function is used to design IIR low-pass, high-pass, band-pass and band-reject filters, and finally load them into the stm32f407 microprocessor. After digital filtering through the stm32f407 master chip, it is finally transmitted back to the host computer via serial communication, and then the waveform results are observed using MATLAB to compare the differences before and after filtering.

To verify the effectiveness of this EMG acquisition filtering system, acquisition verification experiments in two different states were designed. Figure 5 shows the graph of the acquisition test experiment. The subject of the experiment was a 24-year-old male with normal arm muscle groups. The skin of the subject's arm was treated with correlation, and the electrodes were attached to the forearm muscle. The surface EMG data at rest and the action EMG at continuous fist relaxation were measured. The data were transferred to the upper computer via a USB serial transfer assistant to extract the data and subsequently analyzed and processed in MATLAB.

Fig. 5. EMG acquisition system equipment.

IV. Results and Discussion

Spectral analysis of surface electromyography (SEMG) is the process of transforming the SEMG signal from the time domain to the frequency domain for analysis. Its significance lies in the fact that the features of the signal can be revealed after the transformation in the frequency domain even though

the observed signal has no obvious features in the time domain. To obtain information on industrial frequency noise and other disturbances, we need to obtain the spectrum map to analyze it.

The most important algorithm in spectrum analysis is Fast Fourier Transformation (FFT). FFT is a fast algorithm to calculate the Fourier transform and convert discrete time domain signals into discrete frequency domain signals. Compared with the traditional Fourier transform, it has the advantages of fast computation and low complexity.

$$F_n = \frac{(n-1)\times F_s}{N} \tag{9}$$

Using (9), the frequency that *Fn* resolves is Fs/N. If the sampling frequency *Fs* is 1024 Hz, and the number of sampling points is 1024, then it can resolve to 1 Hz. At 1024 Hz of sampling rate, sampling 1024 points takes 1 s. 1 s of sampling time is for signal collection and FFT, then the result can be analyzed to 1 Hz. If the sampling time is 2 s, then the result is analyzed to 0.5 Hz. To increase the frequency resolution, the number of sampling points, that is, the sampling time must be increased.. The frequency resolution and the sampling time are inversely related. After the FFT point *n* is represented by the complex number $a + bi$, then the modulus of this complex number is

$$A_n = \sqrt{a^2 + b^2} \tag{10}$$

The phase is expressed in C code as

$$P_n = a\tan 2(b, a) \tag{11}$$

Based on the above results, it is possible to calculate the expression of the signal corresponding to n points (n ≠ 1 and n <= N/2) as

$$\frac{A_n \times 2}{N} \times \cos(2\pi \times F_n \times t + P_n) \tag{12}$$

For the signal at point *n*=1, which is the DC component, the amplitude is A_1/N. Due to the symmetry of the FFT results, we use the first half of the results, i.e., less than half of the sampling frequency. As shown in Fig. 6, the resting potential of the subject contains severe 50 Hz sinusoidal interference at the industrial frequency when not filtered. Figure 7 shows the time domain diagram of the resting surface EMG signal at 50 Hz and with filtered interference. The figures show that the 50 Hz sinusoidal wave is filtered out completely.

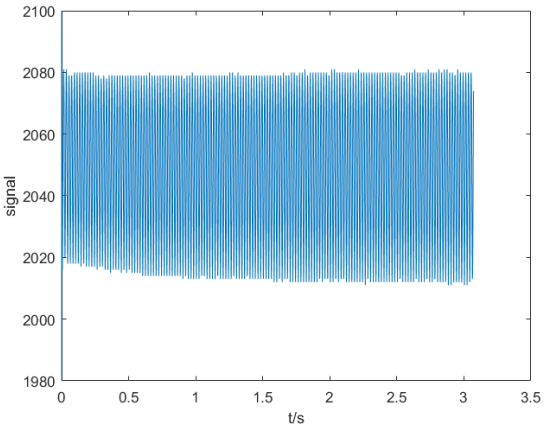

Fig. 6. Raw resting potential.

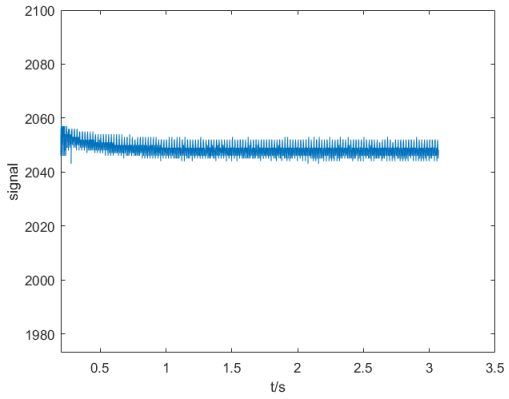

Fig. 7. Resting potential after filtering.

For the transmitted data, this experiment was conducted to analyze and observe the time domain and frequency domain spectrograms before and after filtering. Before filtering, Fig. 7 shows the presence of significant baseline drift due to IDF and low-frequency interference in the time domain. The spectrogram obtained by fast Fourier transform (Fig. 8) shows severe noise interference at 50 Hz. In order to satisfy the demand for the surface EMG signal, the signal was extracted in the range of 20 to 500 Hz, and the unwanted frequency bands and interferences were filtered out. Figure. 9 demonstrates the filtered time domain plot, where the action potential is clearer compared to the original signal. The baseline drift is filtered out, and the effective content is more clearly presented. Figure 10 shows the spectrum plot after low-frequency trap high-frequency filtering, which filters out the 50 Hz industrial frequency interference and successfully extracts the content of the frequency band from 20 to 500 Hz.

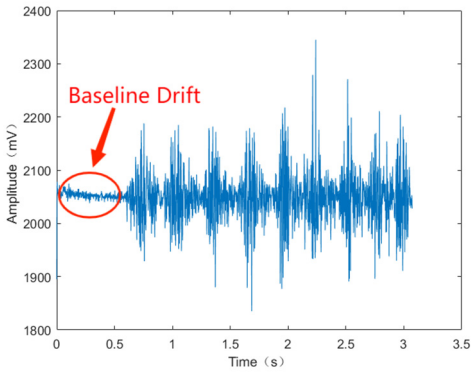

Fig. 8. Raw surface EMG signal.

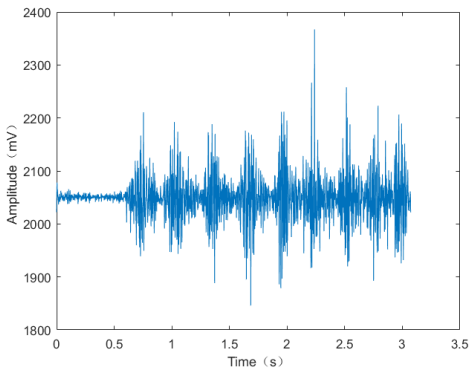

Fig. 9. Surface EMG signal after digital filtering.

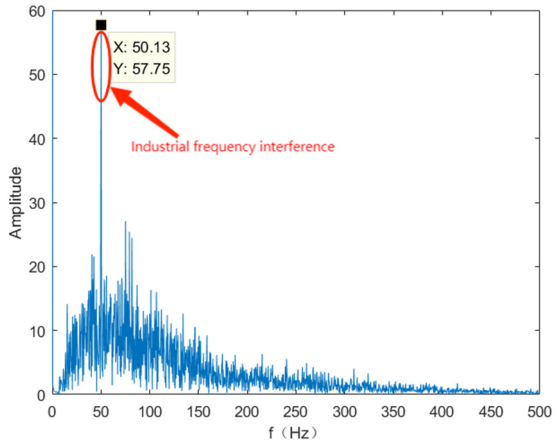

Fig. 10. Original signal spectrum.

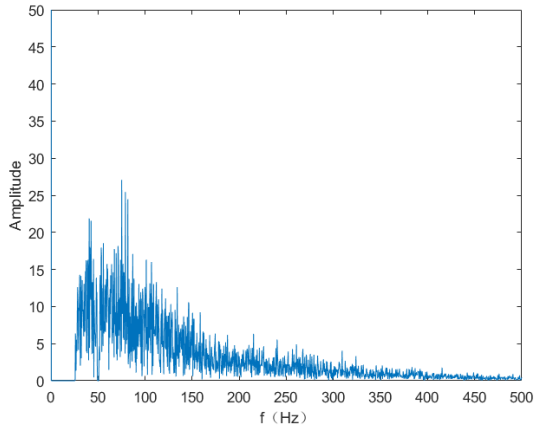

Fig. 11. Filtered spectrum.

V. Conclusion

The designed digital filter is validated by comparing and is verified that it is suitable for processing operations on embedded. The effect of the designed digital filter is also verified by experimental comparison, which achieves -60 dB attenuation of trapped waves at 50 Hz reducing the industrial frequency interference and baseline drift. This system can save hardware resources and simplify the internal circuitry to provide a solution for the miniaturization and portability of surface EMG acquisition devices.

Acknowledgment

This work was supported by the research project of the Fujian Provincial Department of Science and Technology (2019H6024).

References

[1] Jiajia Wu, Xiaoou Li. sEMG Signal Processing Methods:A Review, Journal of Physics Conference Series[J], 2019.06:37-45.

[2] Rozaqi L, Nugroho A, Sanjaya KH, et al. Design of Analog and Digital Filter of Electromyography[C], 2019 International Conference on Sustainable Energy Engineering and Application (ICSEEA). IEEE, 2019:52-67.

[3] Li Shun, Xing Xu Po, Song Chengli. System design and algorithm analysis of surface EMG acquisition signals[J], Software Engineering, 2022, 25(4):5.

[4] Yang ZF, Jue Chen, Mengdie Hu, et al. Design and implementation of digital filters for ECG signals[J], Journal of Hubei University of Nationalities: Natural Science Edition, 2017, 35(1):5.

[5] Chen Xiongbin. Surface EMG signal acquisition and processor design[D]. Guangzhou: South China University of Technology, 2016

[6] Lv P.Y., Guo W.C.,Sheng X.J.,Zhu X.Y.. Design of microarray-based surface EMG acquisition system[J], Joaurnal of Sensing Technology, 2020, 33(6):6.

[7] Feng YQ. Hardware digital filtering technology and its application in telemetry digital seismic acquisition station[D]. Beijing: China University of Geosciences (Beijing), 2011.

[8] Zhou MJ, Wang YY, Ran LY. Implementation of a surface myoelectric signal acquisition device (in English) [J]. Journal of Measurement Science and Instrumentation,2021,12(01):20-26.

[9] Park H. Design and Implementation ofReal-time Electrical Stimulation Artifact Suppression based on STM32[J]. Turkish Journal of Computer and Mathematics Education (TURCOMAT), 2021, 12(5):424-427.

[10] L, Wang K, Liu Z. Design, Development and Testing of a Wearable sEMG Acquisition System[C], 2019 IEEE Intl Conf on Dependable, Autonomic and Secure Computing, Intl Conf on Pervasive Intelligence and Computing, Intl Conf on Cloud and Big Data Computing, Intel Conf on Cyber Science and Technology Congress (DASC/PiCom/CBDCom/CyberSciTech). IEEE, 2019.